Dynamical Downscaling Data for Studying Climatic Impacts on Hydrology, Permafrost, and Ecosystems in Arctic Alaska

5 **Lei Cai[1*], Vladimir A. Alexeev[1#], Christopher D. Arp[2], Benjamin M. Jones[3], Anna Liljedahl[2], Anne Gädeke[2]**

[1]International Arctic Research Center, University of Alaska Fairbanks, 930 Koyukuk Dr. Fairbanks, AK 99775, USA

10 [2]Water and Environment Research Center, University of Alaska Fairbanks, 306 Tanana Loop Rd., Fairbanks, AK 99775, USA

[3]United States Geological Survey, Alaska Science Center, 4210 University Dr. Anchorage, AK 99508-4626, USA

15 [#]Corresponding to: Vladimir A. Alexeev (valexeev@iarc.uaf.edu)

Abstract. Climatic changes are most pronounced in northern high latitude regions. Yet, there is a paucity of observational data, both spatially and temporally, such that regional-scale dynamics are not fully captured, limiting our ability to make reliable projections. In this study, a group of dynamical downscaling products were created for the period 1950 to 2100 to better understand climate change and its impacts on hydrology,

5   permafrost, and ecosystems at a resolution suitable for northern Alaska. An ERA-interim reanalysis dataset and the Community Earth System Model (CESM) served as the forcing mechanisms in this dynamical downscaling framework, and the Weather Research & Forecast (WRF) model, embedded with an optimization for the Arctic (Polar WRF), served as the Regional Climate Model (RCM). This downscaled output consists of multiple climatic variables (precipitation, temperature, wind speed, dew point temperature,

10   and surface air pressure) for a 10 km grid spacing at three-hour intervals. The modeling products were evaluated and calibrated using a bias-correction approach. The ERA-interim forced WRF (ERA-WRF) produced reasonable climatic variables as a result, yielding a more closely correlated temperature field than precipitation field when long-term monthly climatology was compared with its forcing and observational data. A linear scaling method then further corrected the bias, based on ERA-interim monthly climatology,

15   and bias-corrected ERA-WRF fields were applied as a reference for calibration of both the historical and the projected CESM forced WRF (CESM-WRF) products. Biases, such as, a cold temperature bias during summer and a warm temperature bias during winter as well as a wet bias for annual precipitation that CESM holds over northern Alaska persisted in CESM-WRF runs. The linear scaling of CESM-WRF eventually produced high-resolution downscaling products for the Alaskan North Slope for hydrological and ecological

20   research, together with the calibrated ERA-WRF run, and its capability extends far beyond that. Other climatic research has been proposed, including exploration of historical and projected climatic extreme events and their possible connections to low-frequency sea-atmospheric oscillations, as well as near-surface permafrost degradation and ice regime shifts of lakes. These dynamically downscaled, bias corrected climatic datasets provide improved spatial and temporal resolution data necessary for ongoing modeling

25   efforts in northern Alaska focused on reconstructing and projecting hydrologic changes, ecosystem processes and responses, and permafrost thermal regimes. The dynamical downscaling methods presented in this

study can also be used to create more suitable model input datasets for other sub-regions of the Arctic.

Key words: cryosphere, dynamical downscaling, climatic impact, bias correction, Arctic

1. Introduction

Climate change is most pronounced in high latitude regions (Johannessen et al., 2004; Serreze and

5   Francis, 2006; Hinzman et al., 2005).   Although the exact mechanism is still under vivid discussion, Arctic

amplification has been strengthening since the late 1970s, resulting in a stronger surface temperature increase

than at lower latitudes, and thus a more interactive land-surface background of the Arctic (Alexeev et al.,

2005; Serreze and Francis, 2006).

The physical and ecological components of the Arctic are strongly affected by the regional and global

10   climate (Kane et al., 1991; Jorgenson et al., 2010; Grosse et al., 2011; Koven et al., 2011) and this affect is

increasing rapidly (Hinzman et al., 2005; Corell 2006; Barber et al., 2008). For example, permafrost has

warmed by 0.5-4 °C in the western North America Arctic since the 1970s, corresponding with air temperature

increased over the same period (Smith et al. 2010, Romanovsky et al. 2010). Changes in air and ground

temperatures in this region, along with other climatic variable changes and disturbance events, have been

15   linked to permafrost degradation and thermokarst formation (Jorgenson et al., 2006; Lantz and Kokelj, 2008;

Jones et al., 2015), thermokarst lake dynamics and drainage (Plug et al., 2008; Jones et al., 2011; Jones and

Arp, 2015; Lantz and Turner, 2015), thinning winter lake ice growth (Arp et al., 2012) and increases in lake

open water period (Brown and Duguay, 2010), hydrologic changes (Hinzman et al., 1992; Kane, 1997; Lesack

and Marsh, 2007), and changing arctic ecosystems and habitat (Oechel et al., 1993; Hinzman et al., 2005;

20   Tape et al., 2006; Chapin et al., 2012).   Post et al. (2009) reviewed and highlighted that many of the

ecological consequences over the arctic have been underreported except for the abiotic changes, and the

linkage between the climate change and the ecological consequences are still uncertain based on current

studies. One big barrier from better understanding the linkage between the changing climate and the changing

cryosphere are the lack of scale of observation, both on time and space, in the Arctic.

25   Climate observational records are sparsely distributed in the Arctic and typically limited temporally

(Vose et al., 2007). This results from sparsely-distributed observation sites, among which there are even fewer sites that record observation routinely or are well-maintained (Shulski and Wendler, 2007). Observation accuracy is also affected significantly by the harsh Arctic environment (Groisman et al., 1991; Rasmussen et al., 2012). As a result, numerical simulation has become an obvious and powerful alternative. The newest

5   generation of Earth System Models (ESMs) has shown their potential for Arctic climate research, through the complete coupling of each main component of the earth system, as well as global spatial coverage (de Boer et al., 2012; Mortin et al., 2013; Koenigk et al., 2014). Nevertheless, even the latest ESMs use grid spacing of around one degree—far from capable of resolving mesoscale processes like thunderstorms and local land-air interactions, or for use in forcing hydrological models over complex terrains. Therefore,

10   Regional Climate Model (RCM) simulations are also commonly used, in the Arctic in particular. The Weather Research & Forecast (WRF) model has been one widely-used RCM, employed for multiple research projects focusing on specific physical processes in Alaska (Mölders and Kramm, 2010; Cassano et al., 2011; Glisan and Gutowski, 2014; Mölders et al., 2014). However, there is still a lack of RCM products designed specifically for the Alaskan North Slope and with high-resolution spatial and climatic-scale temporal

15   coverage capable of forcing hydrological models.

Our ultimate goal is to better understand climate change and how it impacts hydrology, ecosystems, and permafrost in northern Alaska. RCM simulations represent a favorable tool for building a reasonable climatic background, not only to recapture and project the regional climate, but also to force hydrologic, ecologic, and ground thermal regime models. This paper introduces high-resolution dynamical downscaled data sets

20   made specifically for research applications focused on changing landscapes in northern Alaska for the late 20th century and early 21st century (Fig. 1). Firstly, the Polar Weather Research & Foreacst (Polar WRF) model dynamically downscales both reanalysis data and ESM output, producing high-resolution simulation output for further calibration. Multiple approaches of calibration including the evaluation of model output based on comparing climatology to observation and the bias-correction using linear scaling, thus finalizing

25   the data set specifically made for describing both the historical and projected climatic background over northern Alaska that is capable of serving a multitude of studies and applications tailored to changes occurring

in the cryosphere and the water cycle and ecosystem functioning within the Arctic system.

2. Data sources

Multiple datasets are facilitated in this research, including observational data, reanalysis data, and data from the ESM.

2.1 Polar weather research & forecast (WRF) model

The WRF model is a flexible, state-of-the-art regional atmospheric modeling system (Skamarock et al., 2008). Since previous modeling studies using the polar MM5 model proved that regional optimization is necessary for regional climate simulation over the Arctic region (Brownich et al 2001, Cassano et al 2001), we used the polar WRF, an RCM that originated in the WRF but was upgraded based on regional modeling experiences over the polar region by the Polar Meteorology Group of the Byrd Polar and Climate Research Center at Ohio State University (Hines et al., 2009; Hines et al., 2011). This model includes new parameterization scheme settings and calibrated land-use category profiles designed specifically for modeling both terrestrial and marine component of the Arctic (Hines et al., 2009; Wilson et al., 2011, 2012). Polar WRF version 3.5.1 is used in this study.

2.2 ERA-interim

We chose ERA-interim as the forcing for polar WRF runs. ERA-interim is the latest generation of a reanalysis data set from the European Center for Medium-range Weather Forecast (ECMWF), serving global gridded atmospheric elements (Dee et al., 2011). As an upgraded version of ERA-40, ERA-interim has solved some of the previous data-assimilation problems that led to ERA-40 variable inaccuracy. ERA-interim represents specific progress for hydrological cycles and precipitation fields, which are key factors in determining the quality of WRF runs for this work (Dee et al., 2011). ERA-interim has shown its capability of providing generally better quality gridded climatic variables in high-latitude areas, compared to other reanalysis products (Jakobson et al., 2012, Lindsay et al., 2014).

2.3   Community earth system model version 1 (CESM1)

To obtain downscaled earth system simulation products for the study of regional climate and hydrological features in the 21st century, WRF is forced by Community Earth System Model version 1 (CESM1) (Vertenstein et al., 2011; Taylor et al., 2012) as a second downscaling product. CESM1 is the latest

5   generation of the ESM and a group member of Coupled Model Intercomparison Project Phase 5 (CMIP5) (Taylor et al., 2012). The CESM-WRF simulation is split into two periods, following CESM. "20th Century Ensemble Member #6" is employed as the forcing for the CESM-WRF historical simulation, and "RCP4.5 Ensemble Member #6" as the forcing for the CESM-WRF projected simulation. RCP4.5 (Representative Concentration Pathway 4.5) represents radiative forcing of 4.5 Wm^{-2}, based on the increase in CO_2 emissions

10   from the beginning of 21st century. The latest global mean temperature observations prompted this choice. The observed global temperature of the first decade of the 21st century has indicated a "braking" in the accelerating global warming (Guemas et al., 2013). Other than the RCP8.5 scenario, which assembles uncontrolled greenhouse gas emissions, an observed global mean temperature increase fits more closely with the milder radiative forcing scenarios of RCP2.6 and RCP4.5, which simulate stricter greenhouse gas control

15   policies (Moss et al., 2010; Riahi et al., 2011; Thomson et al., 2011). Although the physical mechanisms of this global warming deceleration and its potential continuity are still under debate, we elected to use a less extreme scenario as the forcing for a projected simulation in this research that will eventually cover the entire 21st century.

2.4   Global historical climatology network daily (GHCN-D)

20   Alongside ERA-interim as a forcing, Global Historical Climatology Network Daily (GHCN-D) data from National Climatic Data Center (NCDC) are chosen as the observational-based reference for the model evaluation of this research (Vose et al., 2007). Alaskan North Slope observational sites, especially those recording long-term climatological data, are sparsely distributed. Only five stations are qualified for routinely-recorded climatic variables north of the Brooks Range in northern Alaska: Barrow, Wainwright,

25   Deadhorse, Nuiqsut, and Umiat (Fig. 2). In this evaluation, we compare their daily precipitation (PRCP),

daily maximum temperature (TMAX), and daily minimum temperature (TMIN).

3. Model initialization

Polar WRF downscaling simulations are conducted for the domain covering the whole North Slope region of Alaska, as well as the Brooks Range to the South and part of the Arctic Ocean to the North (Fig. 2). A ten kilometer grid spacing produces high-resolution climatic variables for northern Alaska. Temporal coverage is set at the same as their forcing—1979-2014 for ERA-WRF, 1950-2005 for CESM-WRF as the historical run, and 2006-2100 as the projected run. The starting point for all runs is the July of their first forcing years. The first six months work as spin-up time, and are not taken into account during data analysis.

Parameterization schemes are set to favor high-resolution, long-term runs. Multiple parameterization schemes are employed for different physical processes. For microphysical processes, the WRF single-moment 5-class scheme (WSM5) is chosen (Hong et al., 1998). The Rapid Radiation Transfer Model (RRTM) (Mlawer et al., 1997) and Dudhia scheme (Dudhia 1996) are used for longwave and shortwave radiation, respectively. The Noah land surface scheme (Noilhan and Planton 1989) is responsible for land surface processes, and the Yonsei University scheme (Hong and Dudhia 2003) parameterizes planetary boundary layer dynamics. Simulations use the Kain-Fritsch convective parameterization (Kain 2004).

Before finalizing all parameterization schemes, multiple one-year-long test runs were done, demonstrating that the double-moment microphysical parameterization scheme produces higher bias for temperature and precipitation during the first half of a year than those for the other. This is due to overestimation of cloud cover, leading to a lack in simulated downward shortwave radiation at the surface. Thus, we decided to select the WSM 5 class instead, a less complicated but more mature microphysical scheme that works reasonably for long-term regional climate modeling (Hong et al., 1998). Particularly for CESM-WRF runs, as WRF does not contain the variable table of CESM data originally, we instead use WRF intermediate files made from CESM by NCAR, available on the CISL Research Data Archive, with data set number DS316.0 (http://rda.ucar.edu/datasets/ds316.0/).

4. Results

4.1 ERA-WRF evaluation

We evaluate model run performance by comparing forcing (ERA-interim), RCM simulation (ERA-WRF), and observations (NCDC GHCN-D) from five stations located in northern Alaska: Barrow, Deadhorse, Nuiqsut, Umiat, and Wainwright. These are the only regional stations with long-term, routinely-recorded climatic variables. We bi-linearly interpolated ERA-interim variables for the stations, and chose the nearest grid points to the stations for WRF variables. This difference in interpolation method was the result of finer grid spacing in WRF than ERA-interim. Specifically for WRF, since three out of five stations are located near the Arctic Ocean, algorithms are revised to pick the nearest points south of the stations, to ensure the chosen points are on land rather than over the ocean.

4.1.1 Monthly climatology

The ERA-interim, ERA-WRF, and NCDC GHCN-D datasets present similar annual precipitation long term intra-annual variation, with more rain in summer and fall than in winter and spring (Fig. 3). WRF and ERA-interim models show more precipitation than observed. Between the two data sets, ERA-interim produces a similar amount or more precipitation annually than WRF, over all five stations except for Barrow, with wet biases varying seasonally. Monthly precipitation climatology for WRF and ERA-interim during the first six months are close, while biases grow in the second half of the year.

Limited by the difficulties in station observations in northern Alaska, accurately measuring winter precipitation has long proven challenging, often leading to underestimation of total precipitation, as most precipitation falls as snow instead of rain, and snow measurement can bias drastically, especially with high wind speed and snow redistribution (Black, 1954; Liston and Sturm, 2002; Rasmussen et al., 2012). These difficulties coincide with observational winter precipitation climatology, yielding close to zero amounts for some of the stations.

Daily maximum temperature (TMAX) and minimum temperature (TMIN) are retrieved from the three-

hourly ERA-WRF output and the six-hourly ERA-interim output to fit NCDC GHCN-D temperature

variables. Since maximum and minimum values for temperature from ERA-interim and WRF are filtered out

from daily temperature with stationary time intervals, while NCDC GHCN-D records truly daily maximum

and minimum temperatures, this manner of extraction may lead to some biases during the comparison.

5   TMAX in ERA-interim and WRF are extracted from the temperature at 0000 UTC (3 pm local time),

while TMAX in NCDC is measured as the true daily temperature maximum. WRF slightly underestimates

TMAX climatologically, compared to observation (Fig. 4). This cold bias is obvious mostly during the

warmest months (June to August) and the coldest months (November to February). The only exception is the

Deadhorse site, at which WRF produces small warm biases (less than 3 K) from February to May. For most

10   stations, ERA-interim also presents cold biases compared to observations, especially in the summer. In winter,

however, cold biases between ERA-interim and observation are generally not as much as those between WRF

and observation.

Similarly, TMIN in ERA-interim and WRF are extracted from the temperature at 1200 UTC (3:00 am

local time). Unlike TMAX, TMIN monthly climatology generally shows a warm bias between ERA-interim

15   and observation, and a cold bias between WRF and observation (Fig. 5). These biases are illustrated year

round, except for March to May, when the cold bias of WRF becomes negligible for all five stations.

TMAX and TMIN jointly reflect the diurnal temperature cycle. ERA-interim is found to have less

diurnal temperature variation over the North Slope. WRF, on the other hand, produces cold biases for both

TMAX and TMIN during the warmest months. However, the TMAX bias of WRF in the winter is so small

20   that it helps even the cold bias of TMIN during the same period, representing a bigger diurnal temperature

variation during the coldest months. Temperature evaluation experiments by the Polar WRF group also found

a cold bias in winter and warm bias in summer on the North Slope since Polar WRF version 3.1.1 (Hines et

al., 2009; Hines et al.; 2011). As found here, these biases remain in version 3.5.1.

4.1.2 Statistical coherence

25   Other than monthly climatology comparisons of precipitation and temperature between observations,

reanalysis data, and RCM simulation, statistics further reveal an in-depth picture of RCM performance. Taylor diagrams are presented for these five stations, showing the correlation coefficients of monthly precipitation (green), TMAX (red), and TMIN (blue) climatology of ERA-interim (✕) and WRF (+) compared to observational data (Fig. 6).

5   Both ERA-interim and WRF demonstrate monthly/seasonal precipitation and temperature variabilities. Correlation coefficients are higher than 0.7 in all cases. Among these three variables, TMAX and TMIN are more closely correlated to observation than is precipitation. Temperature coefficients are all higher than 0.95, while precipitation coefficients are in the range of 0.7 to 0.9. Regarding comparison between data sets, however, WRF-modeled precipitation at these five stations show higher coefficients than ERA-modeled

10   precipitation at Barrow, Wainwright, and Nuiqsut, and similar to Deadhorse and Umiat. The TMIN coefficients are also slightly higher than the TMAX coefficient, especially in comparison between WRF and observations.

     Another important statistical parameter these Taylor diagrams illustrate is normalized standard deviation (STD), representing the monthly/seasonal variability in its reference (observation). Both ERA-interim and

15   ERA-WRF precipitation amounts have a higher standard deviation. The only exception is the STD of ERA-interim precipitation in Barrow, which is similar to observations. Regarding ERA-interim and WRF, WRF produces about 1.5 times the STD of both the ERA-interim and observation. WRF precipitation STDs are higher than those of ERA-interim in Deadhorse and Umiat, while the two differ little in Wainwright and Nuiqsut.

20   Temperature STDs for both ERA-interim and WRF are close to the reference for all stations. Regarding all five stations as a whole, however, TMAX STDs mostly drop on the right side of the reference curve, while TMIN STDs drop to the left of the reference curve in general. This feature reflects the less varied temperature at night than at daytime, for both reanalysis data and the modeling product.

     This statistical feature corresponds quantitatively to the panels in the last section, with higher seasonal

25   variability in WRF monthly precipitation than in ERA-interim, especially during summer. As a result, WRF better captures seasonal precipitation fluctuation, though its climatology deviates a little further than the

ERA-interim from observation. The higher resolution and favorable parameterization schemes in WRF

retrieves, to some extent, the seasonal variability in precipitation over the Alaskan North Slope.

In summary, we evaluate the ERA-WRF simulation by comparing its climatology to the forcing, as well

as to the observational data set. As a result, ERA-WRF has generated a reasonable regional climate for the

5   study region in northern Alaska for the period 1980 to 2014, while greater biases are found in precipitation

relative to temperature. Seasonally, biases are higher in summer and winter than in spring and fall. Before

further application of this product, bias correction is necessary for this data set. Since observations over the

Alaskan North Slope are limited in density and accuracy, the ERA-interim data set instead becomes the

reference in the bias correction process for this research.

10   **4.2 Bias correction**

In order to make this modeled data set useful to further hydrological research, bias correction is essential

for climatic variables. In this case, bias correction is conducted using the linear scaling method (Lenderink

et al., 2007; Teutschbein and Seibert, 2012). A linear scaling method artificially rescales Probability Density

Functions (PDFs), ensuring the corrected monthly climatology corresponds to the reference (ERA-interim,

15   in this case). The formulas for correcting precipitation and temperature differ. The formula for precipitation:

$$P^*_{his}(d) = P_{his}(d)\frac{\mu_m(P_{ref}(d))}{\mu_m(P_{his}(d))}$$

$$P^*_{prj}(d) = P_{prj}(d)\frac{\mu_m(P_{ref}(d))}{\mu_m(P_{his}(d))}$$

in which $P^*_{his}(d)$ and $P^*_{prj}(d)$ are, respectively, daily bias-corrected historical and projected precipitation,

$P_{his}(d)$ and $P_{prj}(d)$ are the originals, $P_{ref}(d)$ is the daily reference precipitation, and μ_m stands for

20   monthly climatology.

The formula for temperature:

$$T^*_{his}(d) = T_{his}(d) + \mu_m(T_{ref}(d)) - \mu_m(T_{his}(d))$$

$$T^*_{prj}(d) = T_{prj}(d) + \mu_m(T_{ref}(d)) - \mu_m(T_{his}(d))$$

Terms in the above formulas are the same as those in precipitation correction equations.

The difference in the bias correction equations for precipitation and temperature is due to their PDFs. Climatologically, daily temperature PDF generally obeys normal distribution, with two tails, while daily precipitation PDF generally obeys two-parameter gamma distribution (Harmel et al., 2002; Hanson and Vogel, 2008). Other variables whose probability density functions behave in the same manner as temperature are

5   bias corrected using the same algorithm. These variables include wind speed, dew point temperature, and surface air pressure. Only precipitation and temperature are considered in this bias correction evaluation, but all variables mentioned above are bias-corrected and included in the completed data set.

4.3 CESM-WRF evaluation

CESM-WRF acts as the second high-resolution data set, as completed for the historical period (1950-

10 2005) and for the projected simulation (2006-2100). CESM-WRF facilitated downscaling for an earth system model describing climatic variability and controlled by its own scenarios, and thus forming a great tool for studying climate change impacts through the end of the 21st century. Like ERA-WRF, this evaluation is also necessary for CESM-WRF.

After linear scaling ERA-WRF precipitation and temperature, we use them as reference for evaluation

15 and bias-correction of CESM-WRF. The overlapping years of ERA-WRF and the historical CESM-WRF run, 1980-2005, represent the comparison period. Firstly, Barrow and Nuiqsut are chosen as the first step of comparison, as Barrow has the best observations on the Alaskan North Slope, for its well-maintained facilities and routinely-recording observations. The site acts as a reference point, representing the climatic features of the North Slope. Further, the data quality for Nuiqsut, located just outside the northeast portion of the Fish

20 Creek Watershed, is critical to the reasonability and accuracy of the hydrological model forced by CESM-WRF runs. The purpose of this evaluation is not only to validate CESM-WRF simulation, but also to produce bias correction parameters that will be used for bias correcting the projected CESM-WRF simulation.

Fig. 7 shows monthly biases for precipitation and temperature at Barrow from 1980 to 2005. The left panel shows biases before bias correction, and the right panel presents biases after applying linear scaling

25 bias correction. For precipitation, original CESM-WRF precipitation has a wetness bias, generally, which is

higher in summer (JJA) than in winter. After bias correction, the plot is distinctly "lighter" in color, indicating

lower biases throughout the period. Statistically, linear scaling drags mean bias down from 0.4681 to 0.0018,

and RMSE down from 0.8135 to 0.3865. Warm biases can be found in monthly mean temperature, occurring

mostly during winter. After bias correction, months with high warm biases (>8 K) decrease from the original.

5   Statistically, mean bias decreases from 1.5729 to 0.4357, and RMSE from 5.1694 to 4.6587.   Fig. 8 includes

the same type of plots as Fig. 7, but for the Nuiqsut station. Precipitation and temperature biases are similar

to Barrow. Linear scaling effectively corrects the wet biases for precipitation and warm biases for temperature.

What is different is that wet biases for precipitation and warm biases for temperature are higher in spring

(MMA) than are those in Barrow. Linear scaling also fixes those successfully.

10   Fig. 9 and Fig. 10 contour seasonal and annual differences in precipitation and temperature between

CESM-WRF and ERA-WRF, both bias corrected. Differences between these two data sets are small:

precipitation differs less than 0.1 mm/day and temperature less than 1 K, showing the reasonability of

dynamical downscaling and the effectiveness of bias correction. CESM-WRF climatology shows a slightly

lower precipitation rate (< 0.02 mm/day) and slightly higher temperature (< 0.4 K) across the study region in

15   northern Alaska. Some seasonal variation features are also found for precipitation and temperature

differences.

Although the bias is small enough for a reasonable modeled data set, seasonal variability is evident in

both the CESM-WRF and the ERA-WRF. CESM-WRF precipitation in spring (Fig. 9) and temperature in

summer (Fig. 10) exhibit opposite features from the annual difference in ERA-WRF. Also, among CESM-

20   WRF, precipitation over mountainous areas and inland lakes remain elevated relative to ERA-WRF. Since

the configuration of these two WRF runs are identical, this small scale fluctuation in precipitation can follow

only from the input field—CESM data. The cause of this heterogeneity in spatial precipitation distribution is

beyond the scope of this paper, although it's interesting to witness how large-scale input causes this

heterogeneous feature for precipitation in WRF.

25   Linear scaling has proven effective for correcting biases but still retaining the short-term variability of

the original CESM-WRF. Bias correction parameters for historical simulation are thus applied for bias

correction on the projected CESM-WRF run. After this, CESM forced dynamical downscaling products for both the historical and the projected periods are completed. These data sets, as well as the reference ERA-WRF simulation, can be applied for various research topics in climatology, hydrology, and ecology over the Alaskan North Slope, thanks to their fine grid spacing and reasonable capture of a set of climatic variables.

5   **5. Discussion**

This paper introduces the birth of two dynamical downscaling products forced by ERA-interim reanalysis data and CESM model output. After computational work was completed, we evaluated these modeled variables and corrected their bias based on ERA-interim climatology and observational datasets. ERA-WRF models produce reasonable precipitation and temperature fields compared to ERA-interim. The

10   mean precipitation amount and the seasonal variability of ERA-WRF are close to those of ERA-interim, though both of them have nearly double the annual precipitation amount relative to observational data. Temperature is, unsurprisingly, simulated better than precipitation. ERA-WRF TMAX and TMIN are especially well-matched to observations throughout the year, although slight cold biases are found, mostly during winter, over the Alaskan North Slope, compared to ERA-interim. On the North Slope, the short and

15   weak solar radiation in winter drag the diurnal solar radiation fluctuation down to a low level, due to the high latitude. This disappearance of variability makes solar radiation less important to driving the daily temperature cycle over the North Slope. On the other hand, cloud cover and wind advection jump out as the important factors for surface temperature, in both summer and winter (Dai et al., 1999; Przybylak, 2000). Winter temperature biases between ERA-WRF and its forcing are possible to dismiss by calibrating

20   parameterizations, and seeking another scheme combination more favorable for resolving clouds and wind in northern Alaska—especially helpful when performing short-term simulations in winter months.

Bias correction is applied to all major climatic variables that are needed to drive future landscape-level modeling efforts in northern Alaska. Bias correction is proven to have good effects in calibrating model product (Fig. 7 & 8). Previous research on CESM1 temperature modeling has found that it underestimates

25   the seasonal cycle over the Arctic, which produces warmer winters and colder summers compared to

reanalysis data does (Walston et al., 2014). CISL RDA ds316.1 applies Reynold averaging of CESM variables, based on ERA-interim that rescales 35-year climatology of CESM but maintains the perturbation term completely (Bruyère et al., 2014; Bruyère et al., 2015). We can assume this underestimation remains in CESM-WRF, brought by its forcing. A linear scaling method for rescaling the monthly climatology/seasonal

5   cycle is applied instead, for better bias corrections than the Reynold averaging method of both ERA-WRF and CESM-WRF. Also, it is notable that not all variables are able to be bias-corrected in this way, and the limitation results from the coarse grid of ERA-interim. For some variables that are not spatially continuous, like the snow depth which is only over the land, the interpolation of variable field from ERA's grid to WRF's grid limits data accuracy over the coastal area, and the fact that ERA's grid does not follow the coast well

10   makes more problematic, since ERA mistakenly recognizes some part of coastal land as part of the ocean, like Barrow. Thus, these kind of variables are not recommended to be bias-corrected before new approach of calibration is developed.

      Linear scaling of CESM-WRF diminished monthly average precipitation and temperature biases, reflect the decreases of mean bias and RMSE. Taking Barrow and Nuiqsut, for example, the original CESM-WRF

15   generally exhibits a wet bias during summer and a warm bias during winter, compared to bias-corrected ERA-WRF (Fig. 7 and Fig. 8). These are also clearly diminished by the bias correction of CESM-WRF. Precipitation correction has a relatively better effect than temperature correction, with both exhibiting virtual biases and statistics. The majority of the climatic variables from both the ERA-WRF and CESM-WRF have been uploaded to the International Arctic Research Center (IARC) Data archive, and are available to

20   download through the FTP server (ftp://climate.iarc.uaf.edu/public_data/WRF/). The IARC Data Archive is a long-term digital storage facility, and a tier-4 member node of the NSF supported DataONE federation of archives. Tier-4 status means that IARC replicates content for other member nodes, in exchange for our content being replicated at member nodes outside of Alaska.

      Spatial variability of temperature climatology over the Alaskan North Slope has been found to be very

25   small due to its relatively flat topography, though precipitation climatology increases from the coast to the interior because of the orographic impediment caused by the Brooks Range (Zhang et al., 1996; Serreze and

Hurst, 2000; Wendler et al., 2009). Comparison between CESM-WRF and ERA-WRF seasonal climatology coincides with this feature, showing some north-to-south gradient for temperature comparison. Precipitation comparison also yields some signals that may be relative to topography, though their existence is still uncertain, as the topographical background is offered by WRF rather than the forcing, and the land-surface

5   backgrounds of these two runs are identical.

The linear scaling method maintains the majority of spatial distribution and temporal climate variability from the original data set, thus retaining their advantage from fine grid spacing and favorability of regional climate impact research. These two dynamical downscaling products, using the polar WRF model and forced respectively by reanalysis data and the earth system model offer major climatic variables, with high spatial

10   resolution over our study domain in northern Alaska (Fig. 2).

6. Applications

The dynamically down-scaled datasets presented in this study provide a framework for enhancing previous research efforts in Northern Alaska. For example, Scenarios Network for Alaska and Arctic Planning (SNAP) offers downscaled high-resolution daily temperature/precipitation based on CMIP3/5

15   GCMs (https://www.snap.uaf.edu/). The Geophysical Institute Permafrost Laboratory model (GIPL) models soil dynamics and offers important variables on permafrost research, such as soil temperature at multiple layers, active layer thickness, freeze-up time, etc. (Marchenko et al. 2008). The GIPL, together with other two ecosystem models, comprise the Integrated Ecosystem Model (IEM), offering various ecosystem projections for all of Alaska and Northwest Canada (Rupp et al., 2015). The previous efforts have been

20   limited by inadequately downscaled and bias-corrected climatic datasets. One shortcoming of the above mentioned model-based data sets is that they are lack of a complete set of climatic variables that coupled with components of atmosphere, land, and ocean, despite of their high resolutions. Some studies that involve surface-air interaction, such as projecting the runoff of a watershed, have to rely on multiple data sets that are independently built from each other. Some inconsistency between variables of atmosphere, land, or ocean

25   therefore may occur. These inconsistency may lead to biases when other numerical simulations are driven by

this dataset.

The downscaled products developed by this study combine the advantages of reanalysis data set/ESM and RCM. It not only downscales the ESM's coarse grid spacing to enable regional climate studies, but also revises its lack of temperature/precipitation variabilities and extremes. Not to mention that it has gridded coverage that offsets the difficulty presented by sparse availability of observations over the Alaskan North Slope. What makes this product outweigh others is that it offers climatic variables from multiple major components of the earth system, including the atmosphere, the land, and the ocean. All the provided variables are reasonably correlated and dependent with each other within the Polar WRF modeling framework. Thus, it is especially suitable for regional climate impacts studies that involves land-air interactions.

Our downscaled and bias-corrected product is being used to drive a grid-based Water Flow and Balance Simulation Model (WaSiM) at watershed scales ranging from 30 to 5,000 km^2 in northern Alaska. Recent droughts, such as occurred in the summer of 2007, along with uncertainty regarding hydrologic intensification (Rawlins et al., 2010) make the use of such hydrologic models valuable for understanding complex climate-permafrost-hydrology interactions (Liljedahl et al. 2016) and for simulating runoff for specific locations which lack gauging records. In the latter case, WaSiM is being applied to a small catchment in the National Petroleum Reserve-Alaska where petroleum development is planned and baseline streamflow records are insufficiently short to evaluate any impact for changes in land-use (i.e., permanent roads, drilling pad, and lake-water extraction for operations) (Heim et al., 2014). Changes in hydrologic connectivity among rivers, streams, and lakes and how this affects fish migration and habitat use is of great interest regarding changes in land-use and even more so regionally with changing or variable climate. Its high-resolution and reasonable precipitation, as well as other key variables, empower the WASiM recapturing the historical and projected variability spatially and temporally over a complex watershed.

Simulation of lake ice growth using temperature and snow depth data from Polar WRF is being compared to multi-temporal synthetic aperture radar (SAR) analysis of lake ice regimes, which is helping to understand changes in sub-lake permafrost, overwintering fish habitat, and availability of winter water supply for industry (Arp et al. 2012). The advantage of using our data set for this analysis is the ability to provide

continuous data for specific regions corresponding to SAR image acquisitions, whereas previous studies using station data often prove very limiting in terms of data gaps and particularly representing snow at a regional distribution. Evidence suggests that shallow lakes along the outer Arctic Coastal Plain are most sensitive to reduced ice growth (Arp et al., 2012; Surdu et al., 2014), yet this proximity is often poorly

5 captured with coarse resolution climate datasets or station data.

Finer grid and optimized parameterization schemes of Polar WRF enable the recapturing of climatic extremes, such as that occurred in 2007 (Jones et al., 2009; Alexeev et al. 2014). Other future studies may include historical and projected extreme climatic events across the North Slope, the projected frequency and intensity of extreme climatic events under the changing climate can impact more than that from the shift of

10 the mean, and the better capability of these downscaling products of capturing the extremes suitably facilitates the extreme study, as well as the teleconnection of low-frequency sea-atmosphere oscillations. The climatic impact to ecosystem is difficult to estimate over the arctic since the lack of detailed the routinely observation (Post et al., 2009). These high-resolution products are able to serve as a high-quality alternative climatic background. The applications may include exploring the degrading permafrost and its deepening active layer

15 to the releasing carbon from underground and vegetation production over the arctic tundra, and then the impact to the habitat change of insects and large animals living based on this arctic environment.

Acknowledgements: Funding for this research is provided by National Science Foundation ARC-1107481 and ARC-1417300. We thank to Andrew Monaghan for converting and sharing CESM data in a WRF

20 intermediate data format. Any use of trade, product, or firm names is for descriptive purposes only and does not imply endorsement by the U.S. Government.

References

Alexeev, V. A., Langen, P. L., and Bates, J. R.: Polar amplification of surface warming on an aquaplanet in

25 "ghost forcing" experiments without sea ice feedbacks, Climate Dynamics, 24, 655-666, 10.1007/s00382-

005-0018-3, 2005.

Alexeev, V. A., Euskirchen, E. S., Cherry, J. E., and Busey, R. C.: Tundra burning in 2007–Did sea ice retreat matter?, Polar Science, 9, 185-195, 2015.

Barber, D., Lukovich, J., Keogak, J., Baryluk, S., Fortier, L., and Henry, G.: The changing climate of the Arctic, Arctic, 7-26, 2008.

Black, R. F.: Precipitation at Barrow, Alaska, greater than recorded, Eos, Transactions American Geophysical Union, 35, 203-207, 1954.

Brown, L. C., and Duguay, C. R.: The response and role of ice cover in lake-climate interactions, Progress in Physical Geography, 34, 671-704, 2010.

Bruyère, C. L., Done, J. M., Holland, G. J., and Fredrick, S.: Bias corrections of global models for regional climate simulations of high-impact weather, Climate Dynamics, 43, 1847-1856, 2014.

Bruyère, C. L., Monaghan, A. J., Steinhoff, D. F., and Yates, D.: Bias-Corrected CMIP5 CESM Data in WRF/MPAS Intermediate File Format, TN-515+STR, NCAR, 27, 2015.

Cassano, J. J., Higgins, M. E., and Seefeldt, M. W.: Performance of the Weather Research and Forecasting Model for Month-Long Pan-Arctic Simulations, Monthly Weather Review, 139, 3469-3488, 10.1175/mwr-d-10-05065.1, 2011.

Chapin III, F. S., Jefferies, R. L., Reynolds, J. F., Shaver, G. R., Svoboda, J., and Chu, E. W.: Arctic ecosystems in a changing climate: an ecophysiological perspective, Academic Press, 2012.

Corell, R. W.: Challenges of climate change: an Arctic perspective, AMBIO: A Journal of the Human Environment, 35, 148-152, 2006.

Dai, A., Trenberth, K. E., and Karl, T. R.: Effects of clouds, soil moisture, precipitation, and water vapor on diurnal temperature range, Journal of Climate, 12, 2451-2473, 1999.

de Boer, G., Chapman, W., Kay, J. E., Medeiros, B., Shupe, M. D., Vavrus, S., and Walsh, J.: A Characterization of the Present-Day Arctic Atmosphere in CCSM4, Journal of Climate, 25, 2676-2695, 10.1175/jcli-d-11-00228.1, 2012.

Dee, D. P., Uppala, S. M., Simmons, A. J., Berrisford, P., Poli, P., Kobayashi, S., Andrae, U., Balmaseda, M.

A., Balsamo, G., Bauer, P., Bechtold, P., Beljaars, A. C. M., van de Berg, L., Bidlot, J., Bormann, N., Delsol, C., Dragani, R., Fuentes, M., Geer, A. J., Haimberger, L., Healy, S. B., Hersbach, H., Hólm, E. V., Isaksen, L., Kållberg, P., Köhler, M., Matricardi, M., McNally, A. P., Monge-Sanz, B. M., Morcrette, J. J., Park, B. K., Peubey, C., de Rosnay, P., Tavolato, C., Thépaut, J. N., and Vitart, F.: The ERA-Interim reanalysis: configuration and performance of the data assimilation system, Quarterly Journal of the Royal Meteorological Society, 137, 553-597, 10.1002/qj.828, 2011.

Dudhia, J.: A multi-layer soil temperature model for MM5, Preprints, The Sixth PSU/NCAR mesoscale model users' workshop, 1996, 22-24,

Gädeke, A., Hölzel, H., Koch, H., Pohle, I., and Grünewald, U.: Analysis of uncertainties in the hydrological response of a model‐based climate change impact assessment in a subcatchment of the Spree River, Germany, Hydrological Processes, 28, 3978-3998, 2014.

Glisan, J. M., and Gutowski, W. J.: WRF summer extreme daily precipitation over the CORDEX Arctic, Journal of Geophysical Research: Atmospheres, 119, 1720-1732, 10.1002/2013jd020697, 2014.

Gooseff, M. N., Balser, A., Bowden, W. B., and Jones, J. B.: Effects of hillslope thermokarst in northern Alaska, Eos, Transactions American Geophysical Union, 90, 29-30, 2009.

Groisman, P. Y., Koknaeva, V., Belokrylova, T., and Karl, T.: Overcoming biases of precipitation measurement: A history of the USSR experience, Bulletin of the American Meteorological Society, 72, 1725-1733, 1991.

Grosse, G., Romanovsky, V., Jorgenson, T., Anthony, K. W., Brown, J., and Overduin, P. P.: Vulnerability and feedbacks of permafrost to climate change, Eos, Transactions American Geophysical Union, 92, 73-74, 2011.

Guemas, V., Doblas-Reyes, F. J., Andreu-Burillo, I., and Asif, M.: Retrospective prediction of the global warming slowdown in the past decade, Nature Climate Change, 3, 649-653, 2013.

Hanson, L. S., and Vogel, R.: The probability distribution of daily rainfall in the United States, Proc. World Environmental and Water Resources Congress, 2008, 1-10,

Harmel, R., Richardson, C., Hanson, C., and Johnson, G.: Evaluating the adequacy of simulating maximum and minimum daily air temperature with the normal distribution, Journal of applied meteorology, 41, 744-

753, 2002.

Heim, K. C.: Seasonal movements of arctic grayling in a small stream on the Arctic Coastal Plain, Alaska, 2014.

Hines, K. M., Bromwich, D. H., Barlage, M., and Slater, A. G.: Arctic land simulations with Polar WRF, Preprints, 10th Conf. Polar Meteorology and Oceanography, 2009, 17-21,

Hines, K. M., Bromwich, D. H., Bai, L.-S., Barlage, M., and Slater, A. G.: Development and Testing of Polar WRF. Part III: Arctic Land*, Journal of Climate, 24, 26-48, 10.1175/2010jcli3460.1, 2011.

Hinzman, L., Kane, D., Gieck, R., and Everett, K.: Hydrologic and thermal properties of the active layer in the Alaskan Arctic, Cold Regions Science and Technology, 19, 95-110, 1991.

Hinzman, L. D., and Kane, D. L.: Potential repsonse of an Arctic watershed during a period of global warming, Journal of Geophysical Research: Atmospheres, 97, 2811-2820, 1992.

Hinzman, L. D., Bettez, N. D., Bolton, W. R., Chapin, F. S., Dyurgerov, M. B., Fastie, C. L., Griffith, B., Hollister, R. D., Hope, A., Huntington, H. P., Jensen, A. M., Jia, G. J., Jorgenson, T., Kane, D. L., Klein, D. R., Kofinas, G., Lynch, A. H., Lloyd, A. H., McGuire, A. D., Nelson, F. E., Oechel, W. C., Osterkamp, T. E., Racine, C. H., Romanovsky, V. E., Stone, R. S., Stow, D. A., Sturm, M., Tweedie, C. E., Vourlitis, G. L., Walker, M. D., Walker, D. A., Webber, P. J., Welker, J. M., Winker, K. S., and Yoshikawa, K.: Evidence and Implications of Recent Climate Change in Northern Alaska and Other Arctic Regions, Climatic Change, 72, 251-298, 10.1007/s10584-005-5352-2, 2005.

Hong, S.-Y., Juang, H.-M. H., and Zhao, Q.: Implementation of prognostic cloud scheme for a regional spectral model, Monthly weather review, 126, 2621-2639, 1998.

Hong, S.-Y., and Dudhia, J.: 17.3 Testing of a new nonlocal boundary layer vertical diffusion scheme in numerical weather prediction applications, 2003.

Jakobson, E., Vihma, T., Palo, T., Jakobson, L., Keernik, H., and Jaagus, J.: Validation of atmospheric reanalyses over the central Arctic Ocean, Geophysical Research Letters, 39, 2012.

Johannessen, O. M., Bengtsson, L., Miles, M. W., Kuzmina, S. I., Semenov, V. A., Alekseev, G. V., Nagurnyi, A. P., Zakharov, V. F., Bobylev, L. P., and Pettersson, L. H.: Arctic climate change: Observed and modelled

temperature and sea‐ice variability, Tellus A, 56, 328-341, 2004.

Jones, B. M., Kolden, C. A., Jandt, R., Abatzoglou, J. T., Urban, F., and Arp, C. D.: Fire behavior, weather, and burn severity of the 2007 Anaktuvuk River tundra fire, North Slope, Alaska, Arctic, Antarctic, and Alpine Research, 41, 309-316, 2009.

5 Jones, B. M., Grosse, G., Arp, C., Jones, M., Walter Anthony, K., and Romanovsky, V.: Modern thermokarst lake dynamics in the continuous permafrost zone, northern Seward Peninsula, Alaska, Journal of Geophysical Research: Biogeosciences, 116, 2011.

Jones, B. M., and Arp, C. D.: Observing a catastrophic thermokarst lake drainage in northern Alaska, Permafrost and Periglacial Processes, 2015.

10 Jones, B. M., Grosse, G., Arp, C. D., Miller, E., Liu, L., Hayes, D. J., and Larsen, C. F.: Recent Arctic tundra fire initiates widespread thermokarst development, Scientific reports, 5, 2015.

Jorgenson, M. T., Romanovsky, V., Harden, J., Shur, Y., O'Donnell, J., Schuur, E. A. G., Kanevskiy, M., and Marchenko, S.: Resilience and vulnerability of permafrost to climate changeThis article is one of a selection of papers from The Dynamics of Change in Alaska's Boreal Forests: Resilience and Vulnerability in

15 Response to Climate Warming, Canadian Journal of Forest Research, 40, 1219-1236, 10.1139/X10-060, 2010.

Kain, J. S.: The Kain-Fritsch convective parameterization: an update, Journal of Applied Meteorology, 43, 170-181, 2004.

Kane, D. L., Hinzman, L. D., and Zarling, J. P.: Thermal response of the active layer to climatic warming in a permafrost environment, Cold Regions Science and Technology, 19, 111-122, 1991.

20 Kane, D. L.: The impact of hydrologic perturbations on arctic ecosystems induced by climate change, in: Global change and arctic terrestrial ecosystems, Springer, 63-81, 1997.

Koenigk, T., Devasthale, A., and Karlsson, K.-G.: Summer Arctic sea ice albedo in CMIP5 models, Atmospheric Chemistry and Physics, 14, 1987-1998, 2014.

Kotlarski, S., Block, A., Böhm, U., Jacob, D., Keuler, K., Knoche, R., Rechid, D., and Walter, A.: Regional

25 climate model simulations as input for hydrological applications: evaluation of uncertainties, Advances in Geosciences, 5, 119-125, 2005.

Koven, C. D., Ringeval, B., Friedlingstein, P., Ciais, P., Cadule, P., Khvorostyanov, D., Krinner, G., and Tarnocai, C.: Permafrost carbon-climate feedbacks accelerate global warming, Proceedings of the National Academy of Sciences, 108, 14769-14774, 2011.

Lantz, T., and Turner, K.: Changes in lake area in response to thermokarst processes and climate in Old Crow Flats, Yukon, Journal of Geophysical Research: Biogeosciences, 120, 513-524, 2015.

Lantz, T. C., and Kokelj, S. V.: Increasing rates of retrogressive thaw slump activity in the Mackenzie Delta region, NWT, Canada, Geophysical Research Letters, 35, 2008.

Lenderink, G., Buishand, A., and Deursen, W. v.: Estimates of future discharges of the river Rhine using two scenario methodologies: direct versus delta approach, Hydrology and Earth System Sciences, 11, 1145-1159, 2007.

Lesack, L. F., and Marsh, P.: Lengthening plus shortening of river‐to‐lake connection times in the Mackenzie River Delta respectively via two global change mechanisms along the arctic coast, Geophysical Research Letters, 34, 2007.

Liljedahl, A. K., Boike, J., Daanen, R. P., Fedorov, A. N., Frost, G. V., Grosse, G., Hinzman, L. D., Iijma, Y., Jorgenson, J. C., and Matveyeva, N.: Pan-Arctic ice-wedge degradation in warming permafrost and its influence on tundra hydrology, Nature Geoscience, 2016.

Lindsay, R., Wensnahan, M., Schweiger, A., and Zhang, J.: Evaluation of seven different atmospheric reanalysis products in the Arctic*, Journal of Climate, 27, 2588-2606, 2014.

Liston, G. E., and Sturm, M.: Winter precipitation patterns in arctic Alaska determined from a blowing-snow model and snow-depth observations, Journal of hydrometeorology, 3, 646-659, 2002.

Mölders, N., and Kramm, G.: A case study on wintertime inversions in Interior Alaska with WRF, Atmospheric Research, 95, 314-332, 10.1016/j.atmosres.2009.06.002, 2010.

Mölders, N., Bruyère, C. L., Gende, S., and Pirhalla, M. A.: Assessment of the 2006-2012 Climatological Fields and Mesoscale Features from Regional Downscaling of CESM Data by WRF-Chem over Southeast Alaska, Atmospheric and Climate Sciences, 04, 589-613, 10.4236/acs.2014.44053, 2014.

Marchenko, S., Romanovsky, V., and Tipenko, G.: Numerical modeling of spatial permafrost dynamics in

Alaska, Proceedings of the ninth international conference on permafrost, 2008, 1125-1130,

Mlawer, E. J., Taubman, S. J., Brown, P. D., Iacono, M. J., and Clough, S. A.: Radiative transfer for inhomogeneous atmospheres: RRTM, a validated correlated‐k model for the longwave, Journal of Geophysical Research: Atmospheres (1984–2012), 102, 16663-16682, 1997.

5   Mortin, J., Graversen, R. G., and Svensson, G.: Evaluation of pan-Arctic melt-freeze onset in CMIP5 climate models and reanalyses using surface observations, Climate Dynamics, 42, 2239-2257, 10.1007/s00382-013-1811-z, 2013.

Moss, R. H., Edmonds, J. A., Hibbard, K. A., Manning, M. R., Rose, S. K., van Vuuren, D. P., Carter, T. R., Emori, S., Kainuma, M., Kram, T., Meehl, G. A., Mitchell, J. F. B., Nakicenovic, N., Riahi, K., Smith, S. J.,

10   Stouffer, R. J., Thomson, A. M., Weyant, J. P., and Wilbanks, T. J.: The next generation of scenarios for climate change research and assessment, Nature, 463, 747-756, http://www.nature.com/nature/journal/v463/n7282/suppinfo/nature08823_S1.html, 2010.

Nelson, F., Shiklomanov, N., Mueller, G., Hinkel, K., Walker, D., and Bockheim, J.: Estimating active-layer thickness over a large region: Kuparuk River basin, Alaska, USA, Arctic and Alpine Research, 367-378,

15   1997.

Noilhan, J., and Planton, S.: A simple parameterization of land surface processes for meteorological models, Monthly Weather Review, 117, 536-549, 1989.

Oechel, W. C., Hastings, S. J., Vourlrtis, G., Jenkins, M., Riechers, G., and Grulke, N.: Recent change of Arctic tundra ecosystems from a net carbon dioxide sink to a source, Nature, 361, 520-523, 1993.

20   Oechel, W. C., and Vourlitis, G. L.: The effects of climate charge on land—atmosphere feedbacks in arctic tundra regions, Trends in ecology & evolution, 9, 324-329, 1994.

Plug, L., Walls, C., and Scott, B.: Tundra lake changes from 1978 to 2001 on the Tuktoyaktuk Peninsula, western Canadian Arctic, Geophysical Research Letters, 35, 2008.

Post, E., Forchhammer, M. C., Bret-Harte, M. S., Callaghan, T. V., Christensen, T. R., Elberling, B., Fox, A.

25   D., Gilg, O., Hik, D. S., and Høye, T. T.: Ecological dynamics across the Arctic associated with recent climate change, Science, 325, 1355-1358, 2009.

Przybylak, R.: Diurnal temperature range in the Arctic and its relation to hemispheric and Arctic circulation patterns, International Journal of Climatology, 20, 231-253, 10.1002/(sici)1097-0088(20000315)20:3<231::aid-joc468>3.0.co;2-u, 2000.

5 Rasmussen, R., Baker, B., Kochendorfer, J., Meyers, T., Landolt, S., Fischer, A. P., Black, J., Thériault, J. M., Kucera, P., and Gochis, D.: How well are we measuring snow: The NOAA/FAA/NCAR winter precipitation test bed, Bulletin of the American Meteorological Society, 93, 811-829, 2012.

Rawlins, M. A., Steele, M., Holland, M. M., Adam, J. C., Cherry, J. E., Francis, J. A., Groisman, P. Y., Hinzman, L. D., Huntington, T. G., and Kane, D. L.: Analysis of the Arctic system for freshwater cycle intensification: observations and expectations, Journal of Climate, 23, 5715-5737, 2010.

10 Riahi, K., Rao, S., Krey, V., Cho, C., Chirkov, V., Fischer, G., Kindermann, G., Nakicenovic, N., and Rafaj, P.: RCP 8.5—A scenario of comparatively high greenhouse gas emissions, Climatic Change, 109, 33-57, 2011.

Riordan, B., Verbyla, D., and McGuire, A. D.: Shrinking ponds in subarctic Alaska based on 1950–2002 remotely sensed images, Journal of Geophysical Research: Biogeosciences, 111, 2006.

15 Romanovsky, V. E., Smith, S. L., and Christiansen, H. H.: Permafrost thermal state in the polar Northern Hemisphere during the international polar year 2007–2009: a synthesis, Permafrost and Periglacial Processes, 21, 106-116, 2010.

Serreze, M. C., and Hurst, C. M.: Representation of mean Arctic precipitation from NCEP-NCAR and ERA reanalyses, Journal of Climate, 13, 182-201, 2000.

20 Serreze, M. C., and Francis, J. A.: The Arctic Amplification Debate, Climatic Change, 76, 241-264, 10.1007/s10584-005-9017-y, 2006.

Shulski, M., and Wendler, G.: The climate of Alaska, University of Alaska Press, 2007.

Skamarock, W. C., Klemp, J. B., Dudhia, J., Gill, D. O., Barker, D. M., Wang, W., Huang, X.-Y., and Powers, J. G.: A description of the advanced research WRF version 3, DTIC Document, 2008.

25 Smith, L. C., Sheng, Y., MacDonald, G., and Hinzman, L.: Disappearing arctic lakes, Science, 308, 1429-1429, 2005.

Smith, S., Romanovsky, V., Lewkowicz, A., Burn, C., Allard, M., Clow, G., Yoshikawa, K., and Throop, J.: Thermal state of permafrost in North America: a contribution to the international polar year, Permafrost and Periglacial Processes, 21, 117-135, 2010.

Tape, K., Sturm, M., and Racine, C.: The evidence for shrub expansion in northern Alaska and the Pan‐

5   Arctic, Global Change Biology, 12, 686-702, 2006.

Taylor, K. E., Stouffer, R. J., and Meehl, G. A.: An overview of CMIP5 and the experiment design, Bulletin of the American Meteorological Society, 93, 485-498, 2012.

Teutschbein, C., and Seibert, J.: Regional climate models for hydrological impact studies at the catchment scale: a review of recent modeling strategies, Geography Compass, 4, 834-860, 2010.

10   Teutschbein, C., and Seibert, J.: Bias correction of regional climate model simulations for hydrological climate-change impact studies: Review and evaluation of different methods, Journal of Hydrology, 456-457, 12-29, 10.1016/j.jhydrol.2012.05.052, 2012.

Thomson, A. M., Calvin, K. V., Smith, S. J., Kyle, G. P., Volke, A., Patel, P., Delgado-Arias, S., Bond-Lamberty, B., Wise, M. A., and Clarke, L. E.: RCP4. 5: a pathway for stabilization of radiative forcing by

15   2100, Climatic Change, 109, 77-94, 2011.

Vose, R., Menne, M., Durre, I., and Gleason, B.: GHCN daily: A global dataset for climate extremes research, AGU Spring Meeting Abstracts, 2007, 08,

Walston, J., Gibson, G., and Walsh, J.: Performance assessment of the Community Climate System Model over the Bering Sea, International Journal of Climatology, 34, 3953-3966, 2014.

20   Wendler, G., Shulski, M., and Moore, B.: Changes in the climate of the Alaskan North Slope and the ice concentration of the adjacent Beaufort Sea, Theoretical and Applied Climatology, 99, 67-74, 10.1007/s00704-009-0127-8, 2009.

Wilson, A. B., Bromwich, D. H., and Hines, K. M.: Evaluation of Polar WRF forecasts on the Arctic System Reanalysis domain: Surface and upper air analysis, Journal of Geophysical Research, 116,

25   10.1029/2010jd015013, 2011.

Wilson, A. B., Bromwich, D. H., and Hines, K. M.: Evaluation of Polar WRF forecasts on the Arctic System

Reanalysis Domain: 2. Atmospheric hydrologic cycle, Journal of Geophysical Research, 117, 10.1029/2011jd016765, 2012.

Yoshikawa, K., and Hinzman, L. D.: Shrinking thermokarst ponds and groundwater dynamics in discontinuous permafrost near Council, Alaska, Permafrost and Periglacial Processes, 14, 151-160, 2003.

5   Zhang, T., Osterkamp, T., and Stamnes, K.: Some characteristics of the climate in northern Alaska, USA, Arctic and Alpine Research, 509-518, 1996.

Zhang, T., Osterkamp, T., and Stamnes, K.: Effects of climate on the active layer and permafrost on the North Slope of Alaska, USA, Permafrost and Periglacial Processes, 8, 45-67, 1997.
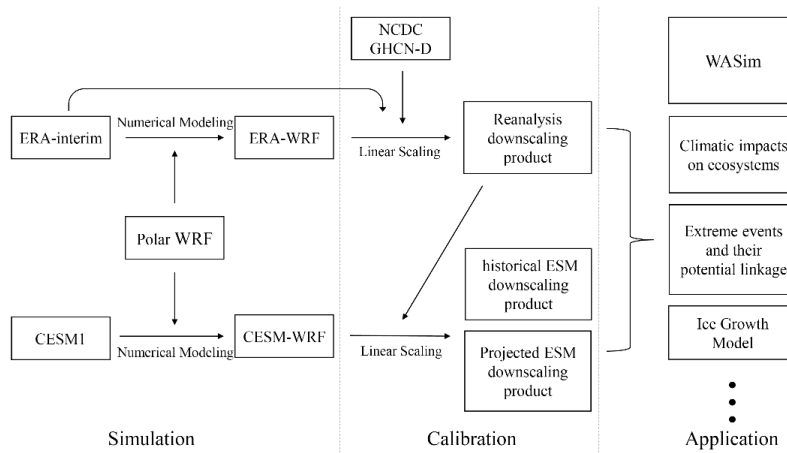
Figure 1: The flowchart of study approach.
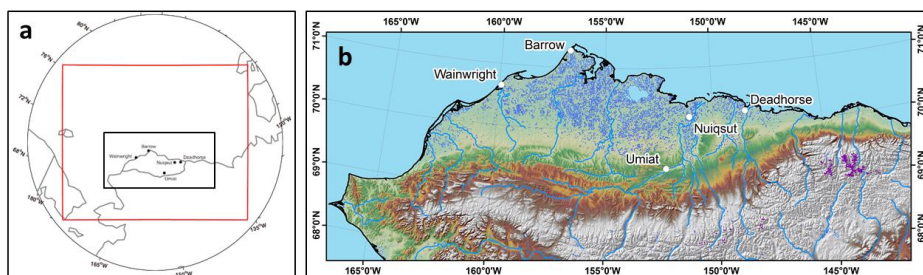
Figure 2: The red box in figure a is the simulation domain, and figure (b) is the detailed topography of the

Alaskan North Slope, which is lined out as the black box in figure (a).
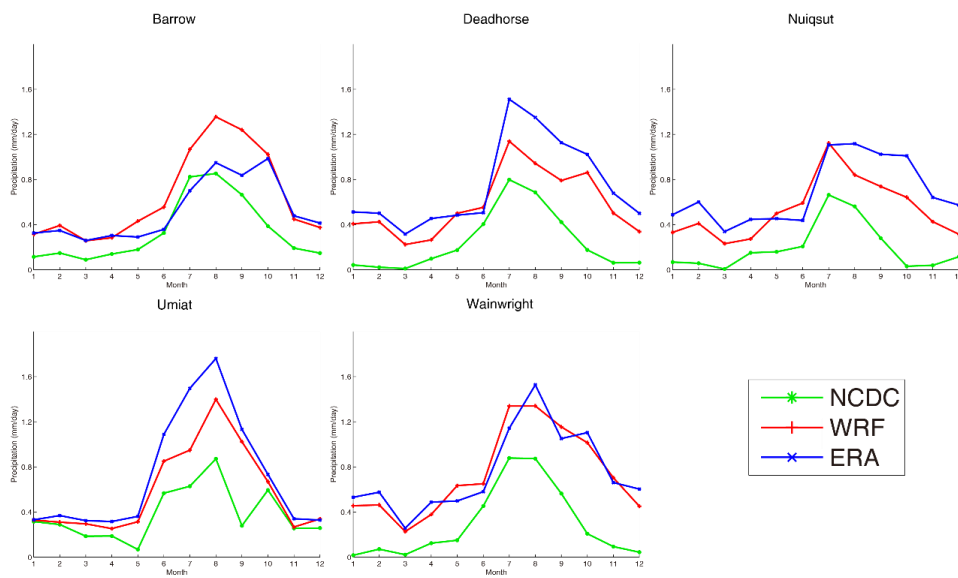
Figure 3: Monthly mean precipitation rate (mm/day) from NCDC (green line), WRF (red line), and ERA-interim

(blue line) at Barrow, Deadhorse, Nuiqsut, Umiat, and Wainwright stations.
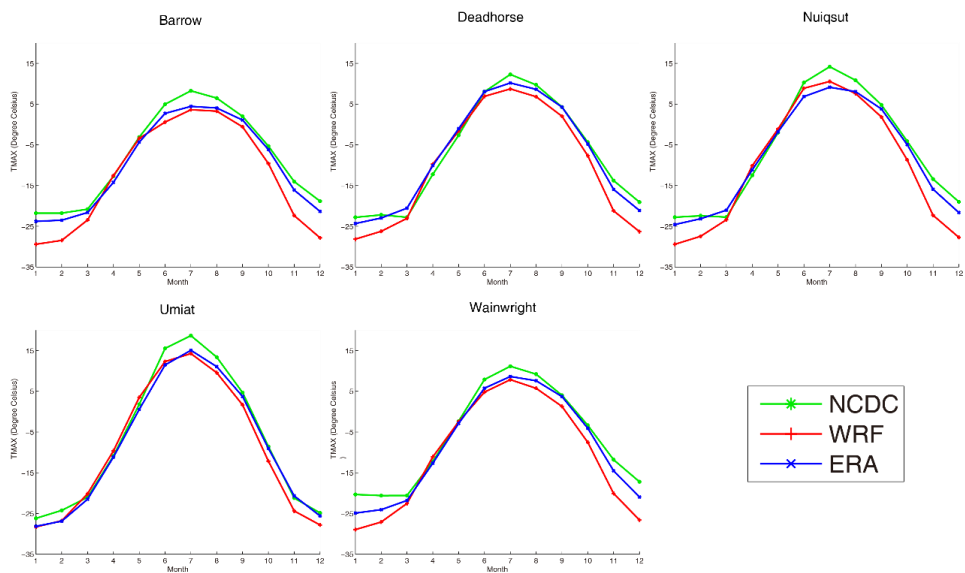
Figure 4: Monthly mean maximum temperature (degree Celcius) from NCDC (green line), WRF (red line), and

ERA-interim (blue line) at Barrow, Deadhorse, Nuiqsut, Umiat, and Wainwright stations.
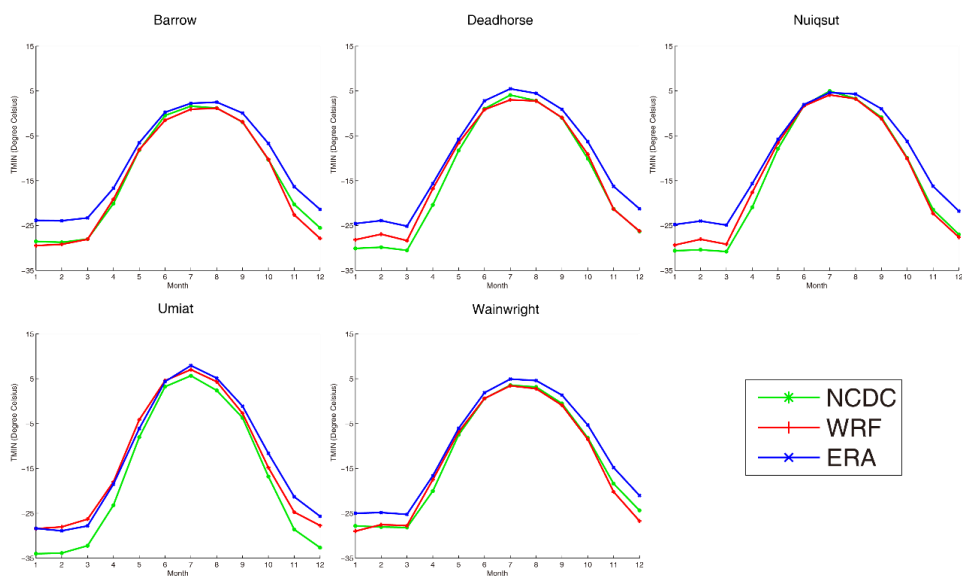
Figure 5: Figure 4: Monthly mean minimum temperature (degree Celcius) from NCDC (green line), WRF (red

line), and ERA-interim (blue line) at Barrow, Deadhorse, Nuiqsut, Umiat, and Wainwright stations.
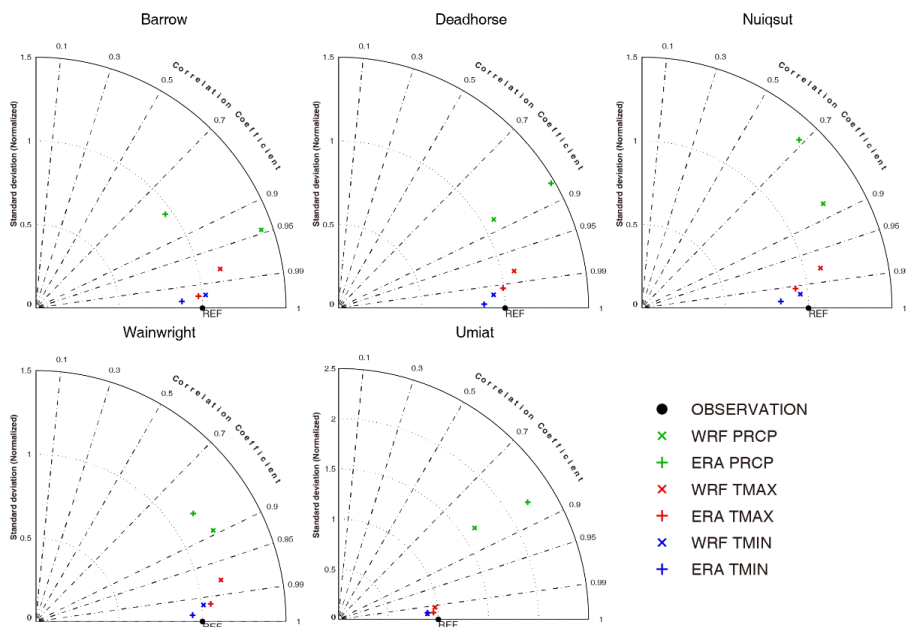
Figure 6: Taylor diagram displaying the correlation coefficients and normalized standard deviations of

precipitation (green), TMAX (red), and TMIN (blue) in the WRF and ERA-interim, compared with

NCDC observational data (black reference dot).
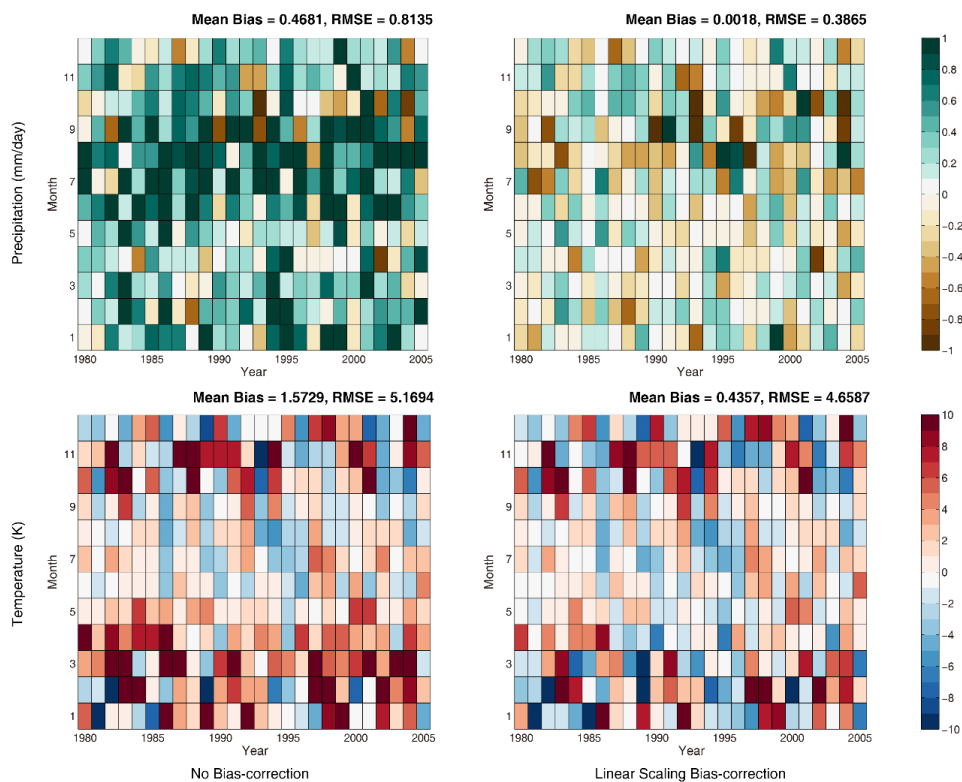
Figure 7: The comparison between differences in raw CESM-WRF and bias-corrected ERA-WRF (left panel), as well as bias-corrected CESM-WRF and bias-corrected ERA-WRF (right panel), for precipitation rate (mm/day, upper panel) and daily mean temperature (K, lower panel) over Barrow, AK.
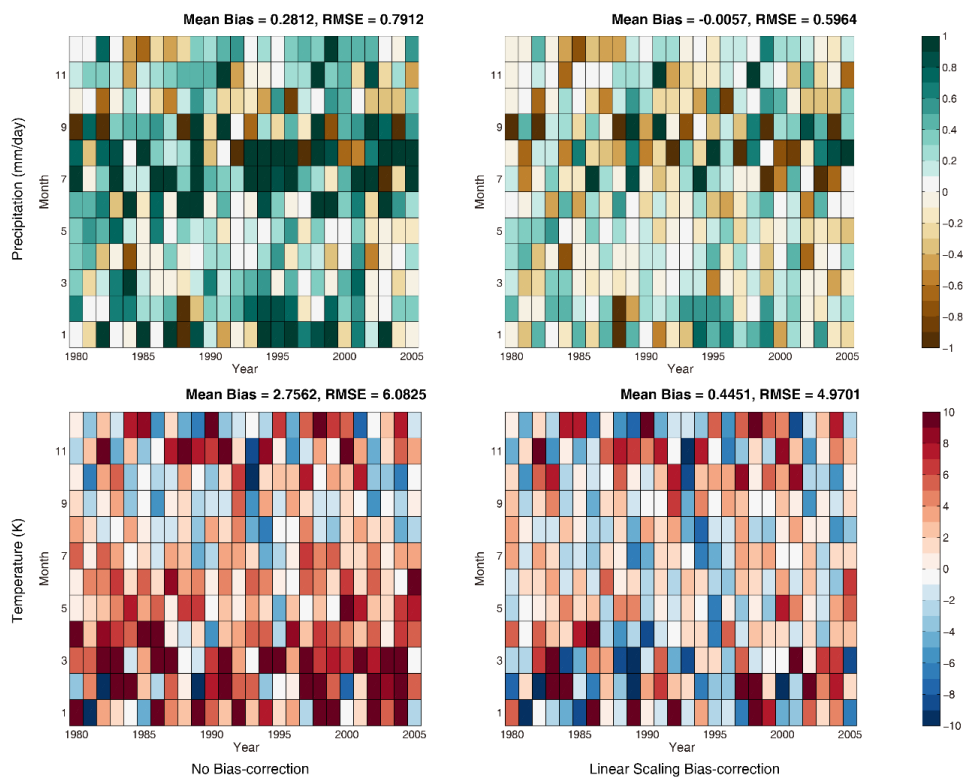
Figure 7: The comparison between differences in raw CESM-WRF and bias-corrected ERA-WRF (left panel), as well as bias-corrected CESM-WRF and bias-corrected ERA-WRF (right panel), for precipitation rate (mm/day, upper panel) and daily mean temperature (K, lower panel) over Nuiqsut, AK.
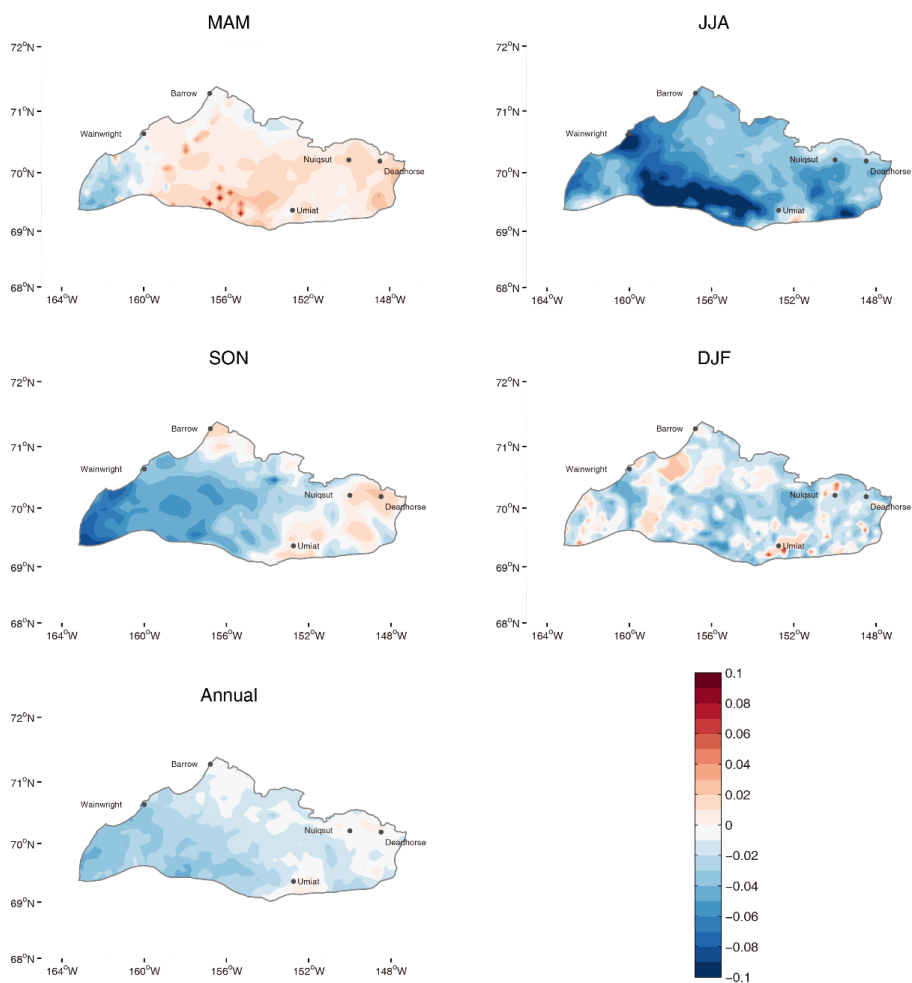
Figure 9: Seasonal and annual differences in precipitation rate (mm/day) between CESM-WRF and ERA-WRF,

both bias-corrected by linear scaling method.
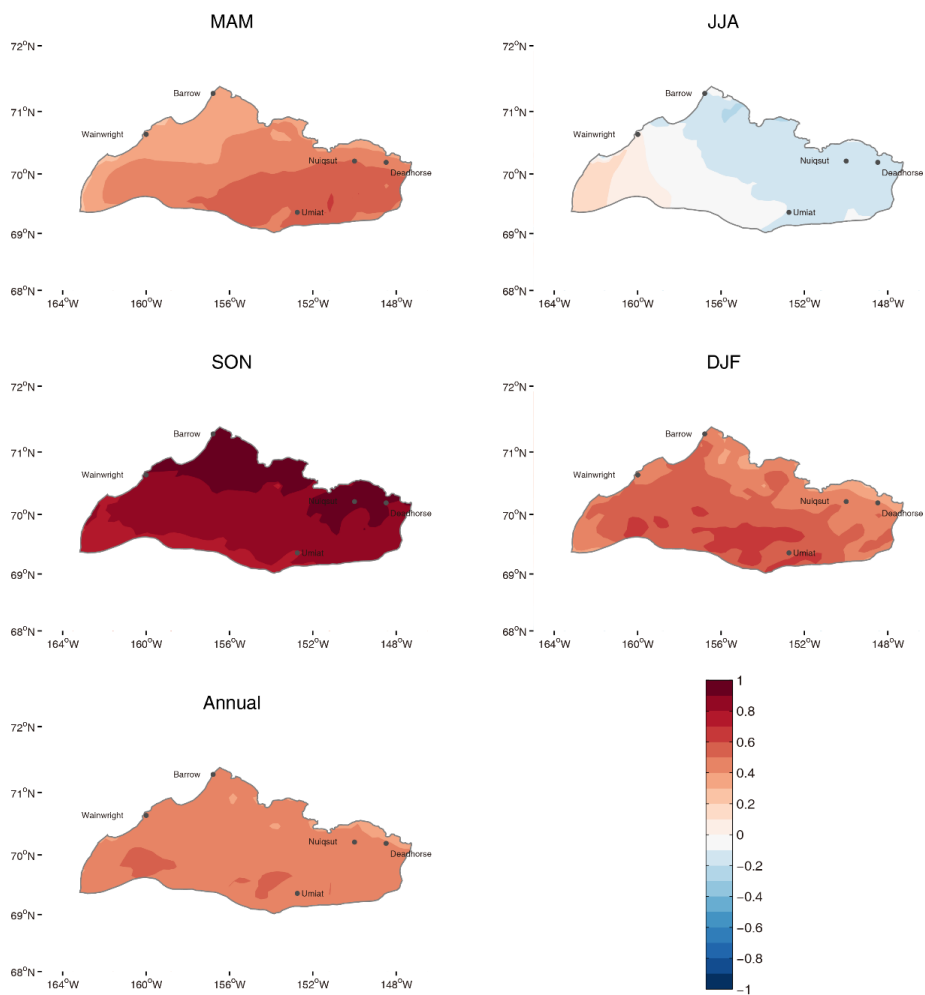
Figure 10: Seasonal and annual differences in daily mean temperature (degree Celsius) between CESM-WRF and ERA-WRF, both bias-corrected by linear scaling method.